Decay of the melt stream during dispersion in granulation devices

Vsevolod I. Sklabinskiy[1], Artem E. Artyukhov[1], Mykola P. Kononenko[1], Jan Krmela[2]

[1] *Sumy State University, Sumy, Ukraine*
[2] *Alexander Dubcek University of Trencin, Trencin, Slovak Republic*

Abstract

The aim of the article is a theoretical description and experimental study of the melt jet expiration process from a perforated shell of a vibrating granulator. Mathematical modeling of hydrodynamic flows was carried out based on the points of classical fluid and gas mechanics and technical hydromechanics. Reliability of the obtained experimental results is based on the application of time-tested in practice methods. Hydrodynamic properties of the liquid jet outflow were obtained. The presented mathematical model allows calculation of the radial component of the jet outflow velocity, as well as determination of the influences of physical and chemical properties of the liquid and the outflow hole diameter on the jet length and flow velocity along the axis to its disintegration into separated drops. The developed mathematical model extended with the theoretical description of the melt dispersion process from rotating perforated shells allowed us to improve design of the granulator to stabilize hydrodynamic parameters of the melt movement. The nitrogen fertilizers melt disperser was investigated regarding industrial-scale production and operating parameters of the process of jet decay into drops, drop size and monodispersity level were optimized.

Keywords: Jet decay, vibration granulator, hydrodynamic of flow movement, melt dispersion process, rotating perforated shell

Available on-line at the Journal web address: http://www.ache.org.rs/HI/

SCIENTIFIC PAPER

UDK: 661.52: 677.021.123.1: 66.099.2

Hem. Ind. **73 (5)** 295-310 (2019)

1. INTRODUCTION

Liquid dispersion processes forming micro- or macro drops are used in power generation, medicine, chemical industry, agriculture and other spheres of human activity. Efficiency of these technological processes and equipment is largely determined by the quality of liquid dispersion, which usually involves obtaining monodisperse drops [1].

This fully applies to the production of the commodity form of nitrogen fertilizers, which is carried out in two main ways [2]:

- granulation starting from the liquid phase by dispersing it on the surface of suspended particles in a fluidized bed that can be variously configured (technologies of Casale S.A., Switzerland; Kahl Group, Germany; Stamicarbon, Netherlands; Toyo Engineering Corporation, Japan; Thyssenkrupp Fertilizer Technology GmbH, Germany, *etc.*) [3-8], including vortex granulation [9,10];
- granulation starting from the liquid phase by dispersing into drops followed by crystallization of the solute by dewatering and cooling (prilling) (devices of Norsk Hydro, Norway; Didier Engineering GmbH, Germany; Imperial Chemical Industries, UK; Kaltenbach-Thuring S. A., France, *etc.*) [11].

In these methods, among others, devices with different forms of a perforated shell, generally being axially symmetrical, can be used for dispersion of the nitrogen fertilizer melt.

Melt dispersion devices can be classified by the form of the working part (*i.e*. perforated shell) and by the presence of internal devices in the perforated shell. Additionally, these devices differ in the nature of force acting on the melt and

Corresponding author: Artem E. Artyukhov, Sumy State University
E-mail: a.artyukhov@pohnp.sumdu.edu.ua
Paper received: 22 April 2019
Paper accepted: 14 September 2019:
https://doi.org/10.2298/HEMIND190422025S

can be static, swirl (tangential introduction of the melt into a perforated shell or to the turbine for the melt spin), and dynamic (rotating) [12].

In recent years, preference is mainly given to conical or cylindrical rotating devices and devices with the cup-shaped shell. This is due to simplicity of operation and high uniformity of resulting liquid drops and commodity granules in comparison to analogue devices.

For example, ammonium nitrate granulators (dispersers), which are currently in operation, provide manufacturing of products with following granulometric composition in terms of mass fraction: 0.5 - 1.5 % of granules < 1.0 mm in size, 90 – 98 % of granules in the size range 2.0 - 4.0 mm, where granules in the size range 2.0 - 2.5 mm comprise 42 – 71 % and granules in the size range 2.0 - 3.0 mm comprise 85 - 95 % [13,14]. Dispersion of melts producing more than 2 % of dust-forming particles of less than 1.0 mm as well as those over 3.5 mm in size, which can be also destructed making dust, leads to dust formation of nitrogenous fertilizers in air in the tower.

In existing equipment, calculation of hydrodynamic characteristics of the liquid jet that is dispersed, is often not performed, resulting in sub-optimal uniformity of the obtained drops [15]. Hydrodynamic parameters of the liquid jet issuing from a single hole or holes of the perforated shell, and design features of devices for fluid dispersion influence the process of jet decay into drops.

The problem of creating the adequate model of jet decay into drops at the opening in a thin wall is highly relevant for dispersion improvement in granulation devices in the mineral fertilizers production. By controlling the jet decay process, we can optimize performance of the disperser and create favorable conditions to produce a product with a high degree of monodispersity.

The aim of the article is a theoretical description and experimental study of the melt jet outflow process from a perforated shell (basket).

2. DESCRIPTION OF THE OBJECT AND METHODS OF RESEARCH

Mathematical modeling of hydrodynamic flows was carried out based on the postulates of classical fluid and gas mechanics and technical hydromechanics [16, 17]. Solving equations of mathematical models was carried out by using the Maple software (Maplesoft, Canada) [18] and the open-source computer algebra system wxMaxima [19, 20]. These systems have been proved to provide reliable and efficient symbolic and numerical algorithms for a wide range of mathematical problems, including a well-known library of numerical algorithms NAG (Numerical Algorithms Group, UK). Adequacy of calculated dependences for the process that was investigated, is validated by the comparison of calculated data with known and experimentally obtained results.

2.1 Experimental rotating vibration granulator

A rotating vibration granulator (manufacturer – Sumy State University, Processes and Equipment of Chemical and Petroleum-Refineries Department, Ukraine; granulator diameter is 560 mm, granulator height is 590 mm) is the main unit of the experimental system (Fig. 1), which consists of a variable perforated membrane 1 with holes to discharge the fluid, housing 2 with a distributive drive 3 and a pipe 4 for introducing air from the fan 5. The housing 2 is also supplied with a fixed liquid distributor 6 with a pipe 7 and a filter element 8.

At the top of the fluid atomizer, a mechanical, electrical or electromagnetic vibrator 9 is installed, which is connected by a rod 10 with the resonator 11 in the form of an elastic disc or plate.

When the granulator is working, liquid that goes through the pipe 7 and the distributor 6 to the bottom part of the granulator flows out of the holes of the perforated membrane. Simultaneously, air at a given pressure is supplied by the fan 5 through the pipe 4 into the cavity of the granulator.

The installation is equipped with a buffer bunker 12 for liquid with a circulation pump 13. Valve 14 and rotameter 15 are used to regulate and measure the liquid flowrate. The oscillations sensor 16 is connected with an oscillograph 17 to observe fluctuations while the digital frequency meter 18 is used to measure the oscillation frequency. When the electro-dynamic or electromagnetic vibrator is used, regulation of oscillations is carried out by the electronic controller 19. A stroboscope (20 and 21) is installed for visual observation of the process of liquid dispersion into drops. Measurements of the liquid pressure in holes and air at the free surface of the liquid are carried out by manometers 22 and 23, respectively. The controller 24 is aimed to regulate the air pressure in the granulator.

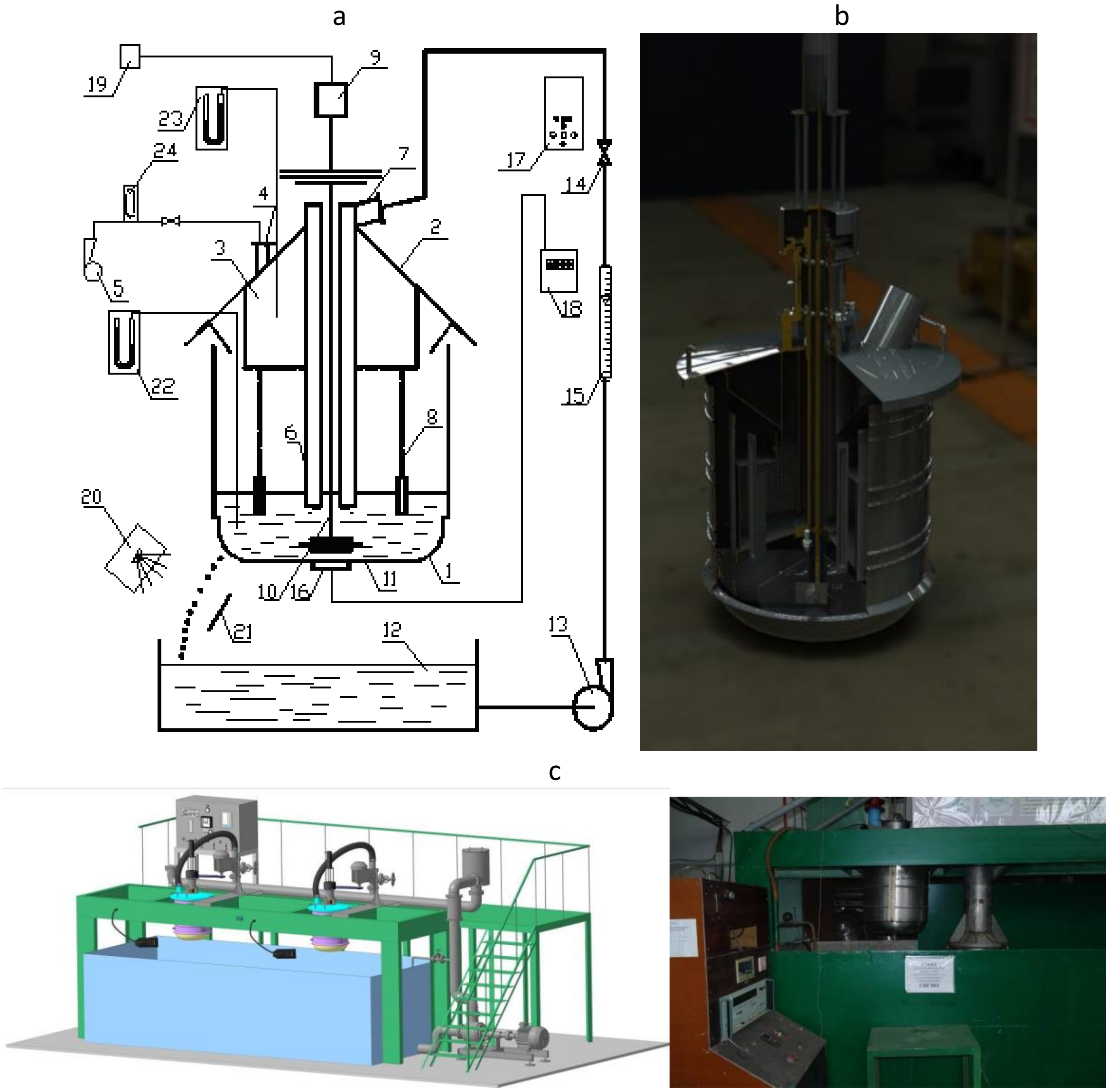

Fig. 1. Experimental installation of the rotating vibration granulator. a) A schematic presentation of the granulator (design features of elements which are not described – see [21]): 1- perforated membrane (diameters of holes are 1.0, 1.1, 1.2, 1.3 and 1.4 mm, number of holes is 1800-2300, bottom shape is toroidal, length is 650 mm, diameter is 560 mm), 2 – housing (height is 590 mm, diameter is 560 mm), 3 – distributive drive, 4 – pipe (diameter is 45 mm), 5 – fan, 6 – liquid distributor, 7 – pipe (diameter is 100 mm), 8 - filter element (metal grid), 9 – vibrator (MFR OTY 77 actuator, range of output frequency 120-1200 is Hz), 10 – rod, 11 - resonator, 12 - buffer bunker, 13 – circulation pump (model Calpeda NC3 25-50/180), 14 – valve, 15 – rotameter (model Raifil RF FM 10), 16 - oscillations sensor, 17 – oscillograph (model C1-65A), 18 – digital frequency meter (model VC3165), 19 – electronic controller, 20, 21 – elements of stroboscope, 22, 23 – manometers (model MT-2У), 24 – controller (model Euroaqua SKD-1); b) 3D model of the vibrating granulator; c) 3D model and a photograph of the experimental installation

Next, the electronic oscillator 19 is switched on and the electrodynamic vibrator 9 started resulting in vibration of the resonator at a certain frequency, which is fixed and recorded by the digital frequency meter 18, which is connected to the vibration sensor 16 of the granulator basket. Air is supplied into the granulator by turning the fan 5 on, and when the interstitial position is changed, the certain pressure is installed based on manometer data. The process of jets dispersion into drops is simultaneously monitored by using a stroboscope 20. When formation of monodisperse drops (without satellite droplets) is observed, measurements are recorded at the manometer 22, which corresponds to the total liquid pressure in the leakage holes, and at the digital frequency meter 18 showing the vibration frequency (upper limit). These liquid and air parameters are varied by changing the vibration frequency by the electronic generator 19 at the lower limit of the granulator stable operation range. Ranges of stable operation are determined for different liquid leakage velocities from holes in the basket, which can be achieved by changing the granulator performance under the constant air pressure or by changing the air pressure by using the pressure regulator at the constant granulator performance. When operating the rotating vibration granulator at different liquid leakage velocities, the fluid flow rate is measured by a graduated cylinder.

Physical modeling is based on methods of the similarity theory. The geometric similarity is maintained by equality of appropriate constants and invariants [22].

The special frequency generator is designed to generate vibration on the radiator of the rotating vibration melting granulator by feeding electric signals of a special shape on the MFR OTY 77 actuator (system operation description - in accordance with [23]).

Main parameters and characteristics:

- frequency range of reproducible oscillations: 200 –1000 Hz
- rated loads: 50 – 100 W
- limits of the permissible relative basic error, setting of the oscillation frequency: 0.5 %
- voltage of the mains supply of the generator: 220±10 V
- frequency of the mains: 60 Hz
- active resistance of the moving coil: 8 Ω
- established trouble-free operating time: 1000 h (with a confidence probability 0,95)

Operating conditions:

- ambient temperature: -10 – 70 °C
- relative humidity: 50 – 80 % at the temperature of 25 °C
- atmospheric pressure: 86 – 106.7 kPa

The special frequency generator consists of:

- Generator of electrical signals of a special form consisting of a block for digital synthesis of frequency, an amplifier and a power supply unit
- Actuator MFR OTY 77

Specifications of the electrical signal generator:

- frequency range: 200 – 1000 Hz
- the minimum frequency setting step is 0.01 Hz
- output power: 60 W
- load resistance: 3.7 Ω
- harmonic coefficient at the frequency of 500 Hz: 0.1 %
- load inductance: 7.3 mH

The digital synthesis unit performs direct digital frequency synthesis (DDS – Direct Digital Synthesizer) and is implemented on a microprocessor. Due to this, the generator has a high frequency stability and a small step of its tuning. The unit allows storing 10 preset frequencies in the non-volatile memory, each of which can be easily changed during operation. Indication of the generated frequency is carried out on the liquid crystal display.

The amplifier provides the necessary amplification of signals from the generator to feed them into a low-resistance load. The amplifier is implemented on an integrated microcircuit. The output stage is made on field-effect transistors, by which performance of a high efficiency amplifier is ensured. The amplifier has a built-in protection system against overload and overheating and a "soft start" system.

To power the whole device a power supply made by the classical transformer scheme is used. Two bipolar rectifiers supply a +/- 12V – the circuit for digital synthesis of frequency, and +/- 24V – amplifier.

Actuator MFR OTY 77: Electromagnetic vibrator consists of a control block and vibro-converter. The control block is used for delivery of a signal of set frequency and amplitude to the vibro-converter. A signal received from the control block, is transferred to the vibro-converter where under the influence of magnetic field a reorientation of crystal lattice of the core alloy material occurs. As a result, the core changes its length. The radiator of granulator's vibrations is joined to the bottom part of the core. Cooling of the vibro-converter is provided by cooling air expulsion. The vibro-system has an input and output signal 4-20 mA which will allow to automatically control the vibration frequency depending on the change of the fusion level in granulator. The control block of the vibro-system is fixed on the central processing unit.

2. 2. Processing of the experimental results

Velocity, V, of the liquid leaking from the granulator holes is calculated as:

$$V = \phi\sqrt{2gH} \quad (1)$$

where ϕ is the discharge coefficient and set to 0.96-0.98 [24].

According to experimental data of upper (f_1) and lower (f_2) limits of the frequency, which provide a monodisperse liquid jet decay, the maximum and minimum lengths of the wave are calculated:

$$\lambda_{max} = V/f_1;\ \lambda_{min} = V/f_2 \quad (2)$$

The melt flowrate, G_S, through the granulator hole is calculated from the measured leaked melt volume, G_τ and time, τ:

$$G_s = G_\tau/\tau \quad (3)$$

Diameter of drops, formed by the decay of liquid jets at the average vibration frequency of the granulator, f_{avi}, is determined from the material balance according to the equation:

$$d_{dr} = \sqrt[3]{\frac{6G_s}{\pi f_{avi}}} \quad (4)$$

The absolute difference of drop diameters and a relative deviation of drop diameters from the average drop diameter at the granulator maximum and minimum productivity are calculated as follows:

$$\Delta d_{dr}^{ab} = d_{dr}^{max} - d_{dr}^{min} \quad (5)$$

$$\Delta d_{dr}^{rel} = \frac{2(d_{dr}^{max} - d_{dr}^{min})}{d_{dr}^{max} + d_{dr}^{min}} \quad (6)$$

To define the optimal number of experiments and the highest accuracy degree and reliability of the obtained results, as well as for the processing of these results, methods of mathematical statistics were used [25].

Two types of measurement errors - random and systematic, may occur during the experiment conducting [26].

A random error reduces the accuracy of experiment results. An analysis of this type of error is possible by using the root-mean-square deviation σ, calculated by the following equation:

$$\sigma = \sqrt{\frac{\sum_{i=1}^{n} \left(\bar{x} - x_i\right)^2}{n-1}} \quad (7)$$

where $\bar{x}$ is the arithmetic mean value; x is the single parameter value; n is the number of measurements.

The maximum possible error of a single measurement, Δ, was determined by the three sigma rule:

$$\Delta = 3\sigma \quad (8)$$

The bilateral confidence interval of the arithmetic mean value ε was determined by the following function [26], provided that this parameter is located in the confidence interval with the probability not less than 95 %:

$$\varepsilon = t\frac{\sigma}{\sqrt{n}} \quad (9)$$

where t is the Student's criterion [27].

The root-mean-square error of indirect measurements is calculated as:

$$\sigma_y = \sqrt{\sum_{i=1}^{n}\left(\frac{\partial y}{\partial x}\Delta x_i\right)^2} \quad (10)$$

where $y = f(x_1, x_2,...x_n)$.

The accuracy of the obtained regression equations is determined by the least-squares method [28].

The systematic measurement error had an identical effect on all parameters that were controlled during the experiment. All measurement devices were calibrated by calibration instruments by comparing their accuracy with that declared in the technical documentation in order to exclude the above error. Connection between measurement devices and controllers was provided with a maximum error of processing signals within 1.5 %.

Creation of graphical dependences was carried out by differential methods of mathematical analysis and integral calculus. Reliability of the obtained experimental results is due to application of time-tested methods in practice.

2. 3. Materials

Melts of ammonium nitrate (agrotechnical chemical; PSC "Azot", Ukraine) and urea (agrotechnical chemical; PSC "Azot", Ukraine) were used. Main parameters of ammonium nitrate and urea are adopted from literature [29].

3. RESULTS AND DISCUSSION

The model of the jet decay is based on the solution of Navier-Stokes equations (11) - (12) and the flow continuity equation (13) in cylindrical coordinates [9], with the following simplifications:

- flow is axially symmetrical;
- cross-section of the jet is circular, there is only jet restriction and extension (the tangential component of jet velocity $\upsilon_\theta = 0$).

$$\upsilon_r\frac{\partial \upsilon_r}{\partial r} = -\frac{1}{\rho}\frac{\partial p}{\partial r} + v\left[\frac{\partial^2 \upsilon_r}{\partial z^2} + \frac{\partial}{\partial r}\left(\frac{\frac{\partial}{\partial r}(r\upsilon_r)}{r}\right)\right] \quad (11)$$

$$\upsilon_z\frac{\partial \upsilon_z}{\partial z} = -\frac{1}{\rho}\frac{\partial p}{\partial z} + v\left[\frac{\partial^2 \upsilon_z}{\partial z^2} + \frac{1}{r}\frac{\partial}{\partial r}\left(r\frac{\partial \upsilon_z}{\partial r}\right)\right] \quad (12)$$

$$\frac{\partial \upsilon_z}{\partial z} + \frac{1}{r}\frac{\partial}{\partial r}r\upsilon_r = 0 \quad (13)$$

By assuming that the axial velocity component at the time of leaving the hole varies parabolically with the radial coordinate:

$$\upsilon_z = A_1r^2z^2 + A_2r + A_3 \quad (14)$$

and transforming the equation (13), we obtain the value of the radial component of the jet velocity:

$$\upsilon_r = \frac{-\frac{1}{2}A_1r^4z + F_1(z)}{r} \quad (15)$$

where $F_1(z)$ is a polynomial function.

Given the fact that the pressure change in a jet in the radial direction is insignificant compared to the axial component, and by substituting (14) into (12) we get:

$$2\left(A_1r^2z^2+A_2r+A_3\right)A_1r^2z=\frac{1}{\rho}\frac{\mathrm{d}p}{\mathrm{d}z}+v\left(2A_1r^2+\frac{4A_1rz^2+A_2}{r}\right) \tag{16}$$

By solving the equation (16) for dp/dz and by integration the expression for pressure change along the jet axis it is obtained:

$$p(z)=-\frac{1}{r}\left(\rho\left(\frac{1}{2}A_1{}^2r^5z^4+A_1r^4z^2A_2+A_1r^3z^2A_3-2\nu A_1r^3z-\frac{4}{3}\nu A_1rz^3-\nu A_2z\right)\right)+C_1 \tag{17}$$

By setting the origin of the coordinate system at the hole exit (z = 0) and by introducing the assumption that the liquid outflow occurs at a constant pressure (p = const), then according to (17) it is obtained that $C_1 = p_1$.

After insertion of this constant we get:

$$p(z)=-\frac{1}{r}\left(\rho\left(\frac{1}{2}A_1^2r^5z^4+A_1r^4z^2A_2+A_1r^3z^2A_3-2\nu A_1r^3z-\frac{4}{3}\nu A_1rz^3-\nu A_2z\right)\right)+p_1 \tag{18}$$

By inserting (18) into (11):

$$\frac{\left(-\frac{1}{2}A_1r^4z+F_1(z)\right)\left(-2A_1r^2z-\frac{-\frac{1}{2}A_1r^4z+F_1(z)}{r^2}\right)}{\mathrm{r}}=$$

$$-\frac{1}{\rho}\left(\frac{1}{r^2}\left(\rho\left(\frac{1}{2}A_1^2r^5z^4+A_1r^4z^2A_2+A_1r^3z^2A_3-2vA_1r^3z-\frac{4}{3}vA_1rz^3-vA_2z\right)\right)\right)- \tag{19}$$

$$-\frac{1}{r}\left(\rho\left(\frac{5}{2}r^4A_1^2z^4+4A_1r^3z^2A_2+3A_1r^2z^2A_3-6vA_1r^2z-\frac{4}{3}vA_1z^3\right)\right)+v\left(\frac{1}{r}\frac{\mathrm{d}^2F_1(z)}{\mathrm{d}z^2}-4A_1rz\right)$$

we obtain the differential equation of total derivatives in respect to the function $F_1(z)$. Based on the fact that the derivative dυ_r/dz is equal to:

$$\frac{\mathrm{d}\upsilon_r}{\mathrm{d}z}=\frac{-\frac{1}{2}A_1r^4z+\frac{\mathrm{d}F_1(z)}{\mathrm{d}z}}{r} \tag{20}$$

and the radial velocity component of the jet at z=0 becomes υ_r=0, we obtain:

$$\frac{1}{2}A_1r^4z=\frac{\mathrm{d}F_1(z)}{\mathrm{d}z} \tag{21}$$

By using the boundary conditions F_1(z = 0) =0 and dF_1/dz (z = 0) =0, and putting them into the equation (14) we obtain the value of the function F_1 as a polynomial:

$$F_1(z)=\frac{1}{6}\frac{(-A_2+8A_1r^3)z^3}{r}+\frac{1}{48}\frac{A_1r^2(3A_1r^4-12A_2r-8A_3)z^4}{\nu} \tag{22}$$

Substituting the relation (22) in the equation (15) leads to:

$$\upsilon_r=\frac{1}{48}\frac{z\left(-24A_1r^5v-8vz^2A_2+64vz^2A_1r^3+3A_1^2r^7z^3-12A_1r^4z^3A_2-8A_1r^3z^3A_3\right)}{vr^2} \tag{23}$$

The coefficient A_2 can be found by assuming that on the jet surface $r = r_s$ the pressure p is equal to the pressure of the surrounding environment p_0. This boundary condition can be written as:

$$p_0=-\frac{1}{r_s}\left(\rho\left(\frac{1}{2}A_1^2r_s{}^5z^4+A_1r_s{}^4z^2A_2+A_1r_s{}^3z^2A_3-2vA_1r_s{}^3-\frac{4}{3}vA_1r_sz^3-vA_2z\right)\right)+p_1 \tag{24}$$

Thus, the coefficient A_2 is now calculated as:

$$A_2=-\frac{1}{6}\frac{(r_s(3z^4A_1^2\rho r_s{}^4+6z^2A_1\rho r_s{}^2A_3-12zA_1\rho vr_s^2-8\rho vA_1z^3-6p_1+6p_0))}{\rho z(A_1r_s{}^4z-v)} \tag{25}$$

The coefficient A_3 can be defined by assuming that that if r=0, υ_r=0:

$$A_3=-\frac{1}{6}\frac{3z^4A_1^2\rho r_s{}^4+6p_0-12zA_1\rho vr_s{}^2-8\rho vA_1z^3-6p_1}{z^2r_s^2\rho A_1} \tag{26}$$

Accordingly,

$$\upsilon_z = A_1r^2z^2-\frac{1}{6}\frac{3z^4A_1^2\rho r_s{}^4+6p_0-12zA_1\rho vr_s{}^2-8\rho vA_1z^3-6p_1}{z^2r_s^2\rho A_1} \tag{27}$$

The coefficient $A_1$is determined by assuming that at a point close to the origin of the coordinate system $z = z_0$, the exhaust velocity has not yet changed its value and is equal to the flow velocity jet in the hole $\upsilon_z = \upsilon_{z_0}$ that is:

$$\upsilon_{z_0}=\frac{1}{6}\frac{6A_1^2r^2z_0^4r_s^2-3z_0{}^4A_1^2\rho r_s{}^4-6p_0-12z_0A_1\rho vr_s{}^2+8\rho vA_1z_0{}^3+6p_1}{z_0{}^2r_s^2\rho A_1} \tag{28}$$

When we solve the resulting equation (28) for the coefficient A_1, we obtain:

$$A_1=\frac{1}{3}\frac{1}{z_0^3r_s^2\rho(2r^2-r_s{}^2)}(-4\nu\rho z_0^2+3\upsilon_{z_0}r_s^2\rho z_0-6\rho\nu r_s^2+(16\nu^2\rho^2z_0^4-24\nu\rho^2z_0^3\upsilon_{Z0}r_s^2+48\nu^2\rho^2z_0^2r_s^2+$$
$$+9\upsilon_{z_0}^2r_s^4\rho^2z_0^2-36\upsilon_{z_0}r_s^4\rho^2z_0\nu+36\rho^2\nu^2r_s^4+36z_0^2r^2r_s^2\rho p_0-36z_0^2r^2r_s^2\rho p_0-36z_0^2r^2r_s^2\rho p_1-$$
$$-18z_0^2r_s^4\rho p_0+18z_0^2r_s^4\rho p_1)^{1/2}) \tag{29}$$

The presented mathematical model allows calculating radial and axial components of the velocity jet outflow, as well as to establish the influence of physical and chemical properties of the liquid and the hole diameter on the jet length and velocity along the axis to its disintegration into separate drops (Figs 2 and 3).

The radial component of the velocity scarcely appears at a short distance from the hole. When the distance increases, radial flows in the jet appear, which cause its breaking-up into drops. It is indicated by the significant increase of the radial component. Increases in the temperature of the melt and the diameter of the perforated shell hole lead to the reduction of the distance from the hole, at which the radial component becomes critical that is at which the jet is broken up. The negative velocity indicates the break off of the flow (detachment of the jet with the formation of the vortex flows), which disappears with an increase of parameter z.

The smaller the distance from the outflow hole during jet breaking-up, the smaller the length of the jet portion, which forms the drop volume during jet breaking-up. This hypothesis coincides with the results of other scientists' studies [30].

For the granulator basket rotation velocity of n = 60 rpm and a load of 37 t/h optimal diameter of the hole is d = 1.2 mm and the melt temperature is 185 °C.

An example of comparison of theoretical calculations and experimental results of velocity radial component measurement is shown in Table 1.

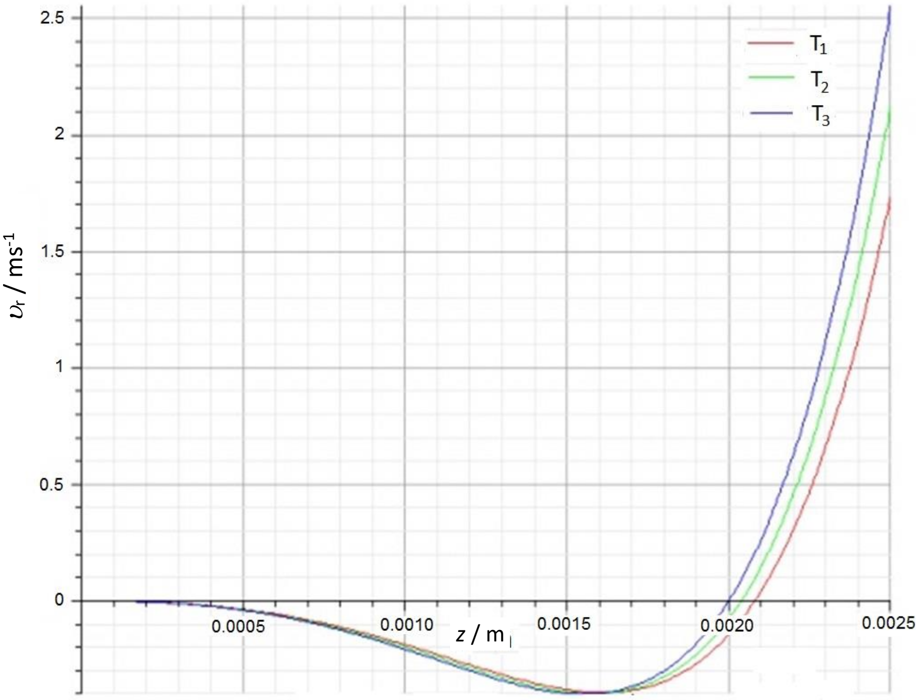

Fig. 2. Dependence of the radial component of the jet velocity of the ammonium nitrate melt on the axial distance, z, from the hole 1.3 mm in diameter at different temperatures of the melt at T_1 = 175°C, T_2 =180°C, T_3 = 185°C and the vibration frequency of 340 Hz (viscosities were 5.36, 5.03, 4.74 mPa·s, densities were 1434, 1431, 1428 kg/m^3 respectively)

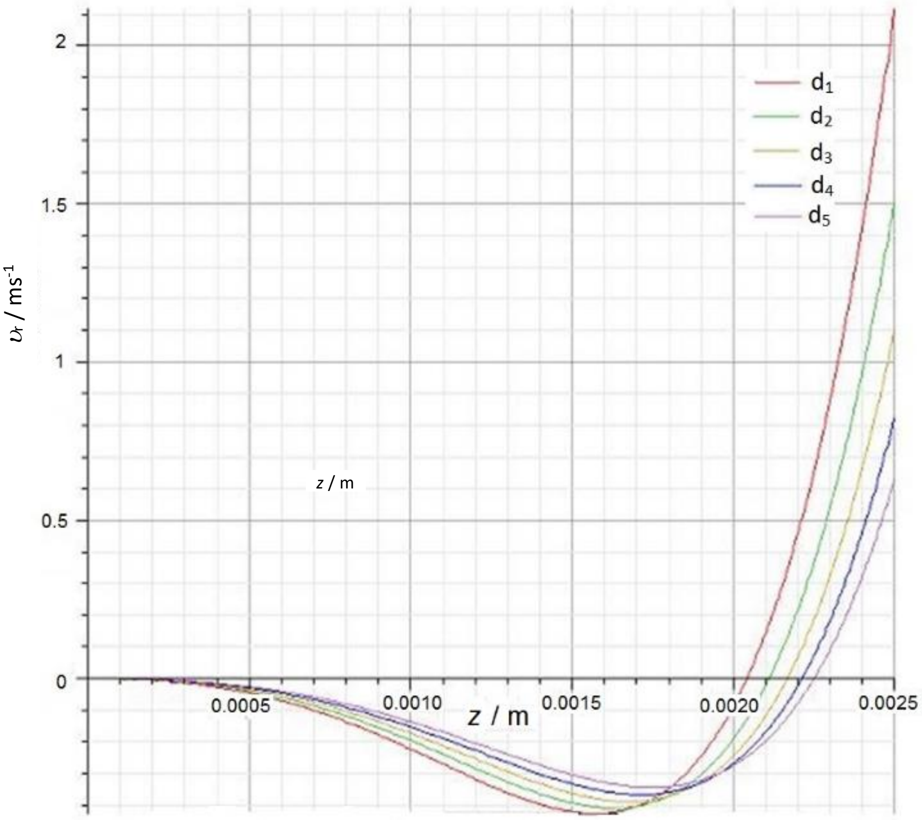

Fig. 3. Dependence of the radial component of the jet velocity of the ammonium nitrate melt on the axial distance, z, from the holes of different diameters: d_1=1.0 mm, d_2=1.1 mm, d_3=1.2 mm, d_4=1,3mm, d_5=1,4 mm at the temperature of 185 °C (viscosity was 4.74 mPa·s, density was 1428 kg/m^3) and the vibration frequency of 340 Hz

Consider the following form of Table 1: Basket tests of the granulator (shown in Fig. 1) confirmed the theoretical research and provided a basis for modernization of the equipment construction. During the tests, a stable jet breakup into drops at a distance of 2-5 mm from the wall of the perforated shell was obtained (Figs 4, 5).

Table 1. An example of comparison of theoretical calculations and experimental results of υ_r measurement (hole diameter was 1.3 mm, temperatures of the melt was 175 °C (viscosity was 5.36 mPa·s, density was 1434 kg/m^3), vibration frequency was 340 Hz, granulator basket rotation velocity was n = 60 rpm and a load was 37 t/h)

$\upsilon_{r.theor}$ / m s^{-1}	No of measurement	$\upsilon_{r.exp}$ / m s^{-1}	$\upsilon_{r.theor}$ / m s^{-1}	No of measurement	$\upsilon_{r.exp}$ / m s^{-1}
	z = 0 m			*z*= 0.0005 m	
0	1	0	-0.05	1	-0.04
0	2	-0.003	-0.05	2	-0.02
0	3	0.002	-0.05	3	-0.08
0	4	0	-0.05	4	-0.07
0	5	0.004	-0.05	5	-0.09
0	6	-0.005	-0.05	6	-0.04
	z = 0.001 m			*z* = 0.0015 m	
-0.2	1	-0.21	-0.4	1	-0.4
-0.2	2	-0.19	-0.4	2	-0.42
-0.2	3	-0.19	-0.4	3	-0.39
-0.2	4	-0.19	-0.4	4	-0.38
-0.2	5	-0.18	-0.4	5	-0.4
-0.2	6	-0.2	-0.4	6	-0.41
	z = 0.002 m			*z* = 0.0025 m	
0	1	-0.01	2.5	1	2.44
0	2	0.01	2.5	2	2.53
0	3	0.02	2.5	3	2.51
0	4	0	2.5	4	2.41
0	5	-0.03	2.5	5	2.56
0	6	0	2.5	6	2.6

a

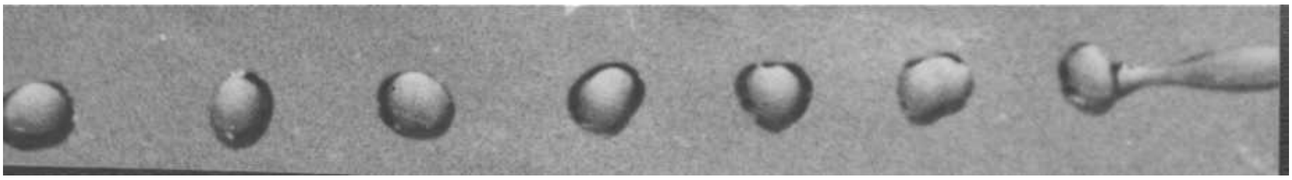

b

Fig. 4. Jet disintegration into drops after the outflow from the perforated shell: a) ammonium nitrate drops, vibration frequency of 200 Hz; b) ammonium nitrate drops, vibration frequency of 340 Hz. Diameter of the hole was 1.1 mm and the temperature was 185°C (viscosity was 4.74 mPa·s, density was 1428 kg/m^3). Granulator basket rotation velocity was n = 60 rpm and a load of 37 t/h

The developed mathematical model was extended with the theoretical description of the melt dispersion process from rotating perforated shells, which allowed us to improve the granulator design to stabilize hydrodynamic parameters of the melt movement within it. By applying of a weighted vortex layer in combination with the vibrating material liquid spray and rotation of liquid jets by their decay should further improve the quality of the granulated product.

A scheme of the modernized granulator is shown in Fig. 6, and layout solutions for the granulator installation in a granulation tower in Fig. 7. Similarity of respective particles movements and their trajectories in the industrial design and in the experimental granulator is maintained.

Fig. 5. Steady jet disintegration into drops after the outflow from the perforated shell: ammonium nitrate drops, vibration frequency of 340 Hz. Diameter of the hole was 1.1 mm and the temperature was 185°C (viscosity was 4.74 mPa·s, density was 1428 kg/m³). Granulator basket rotation velocity was n = 60 rpm and a load of 37 t/h

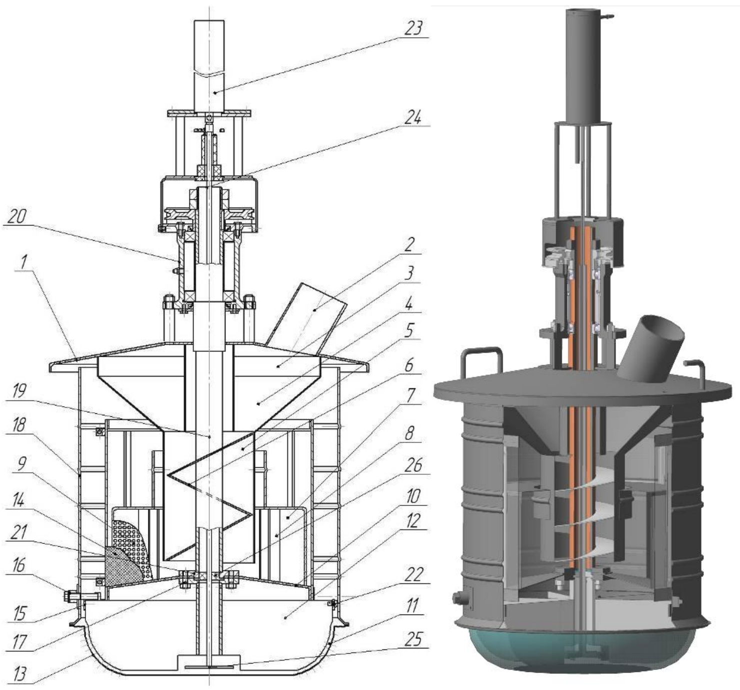

Fig. 6. The improved rotating vibration granulator of solutions (melts): 1 - housing; 2 - pipe for introducing the solution (melt); 3 - ring collector; 4 - reverse cone; 5 - annular channel; 6 - auger; 7 - distributor of the solution (melt); 8 - directing blades; 9 - perforated cylinder; 10 - directing cone for the solution (melt); 11 - perforated bottom (basket); 12 - pressure blades; 13 - hole; 14 - mesh for the final melt filtration; 15 - ring; 16 - bolts; 17 - pins; 18 - cylindrical chamber; 19 - hollow shaft; 20 - bearing assembly; 21 - flange connection; 22 - bulge for centering the cylindrical chamber; 23 - vibration device; 24 - rod; 25 - disc radiant; 26 - hub.

The improved granulator has a guiding element in the form of an auger installed, so when the melt contacts the shoulder blade, the total melt pressure is increased by transforming the screw mechanical energy into the melt kinetic energy and then turning it into the internal energy. Possibility of screw rotation provides an option for increasing the pressure in front of the outflow holes.

Pilot testing of the improved granulator of the total capacity of 37 t/h in production of ammonium nitrate at different climatic conditions (humid and hot climate, temperate continental climate) showed a high yield of marketable fractions and reduction of dust content in flue gases. High level of monodispersity of granules is achieved by improving the fusion hydrodynamics in the granulator and by applying vibration to the jets leaking from the basket perforated bottom. Also, the improved granulator significantly reduced the dust level in the air leaving the tower. Axial flow fans capture from 16 to 38 mg/m^3 of dust so that the granulator enables reduction of costs needed for purchasing expensive new equipment for treatment of the exhaust air.

Results of basic tests of the improved granulator are shown in Figs 8 and 9. Analysis of Figures 8 and 9 provides determination of an optimal (operating) vibration frequency (frequency range), at which the maximal degree of drop monodispersity is achieved. At these conditions, the melt jet disintegrates evenly and without formation of drop satellites.

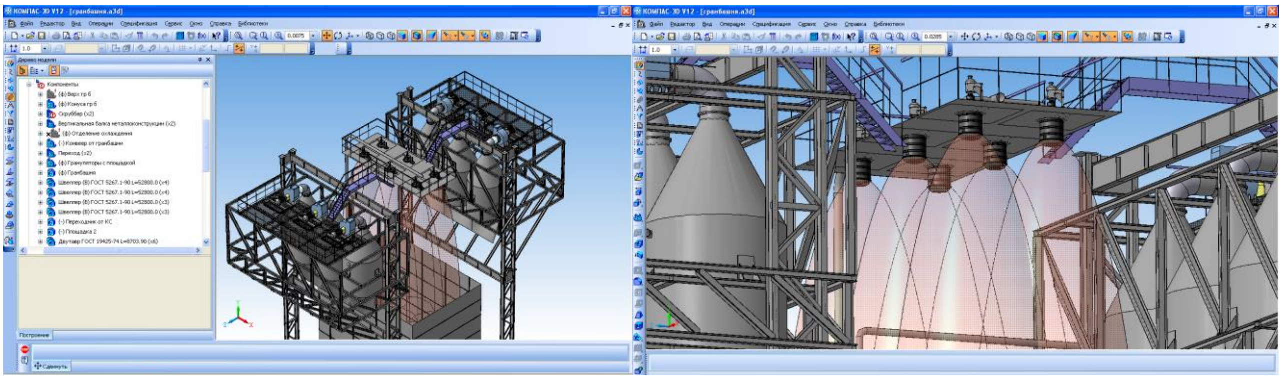

Fig. 7. Layout solutions for granulator installation in a granulation tower

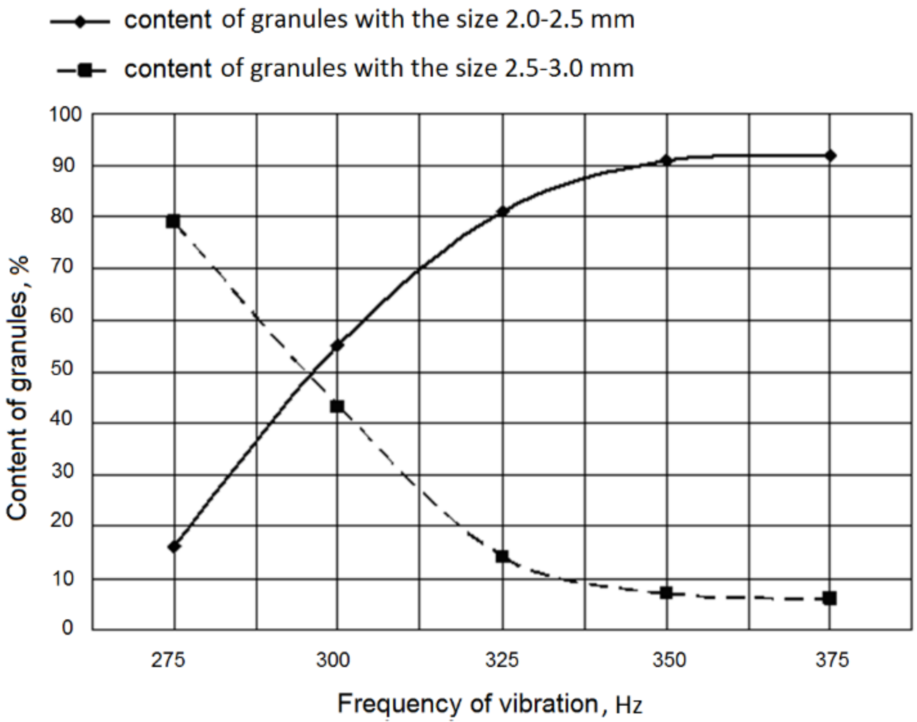

Fig. 8. Mass fractions of ammonium nitrate granules with sizes 2.0 – 2.5 mm and 2.5 - 3.0 mm as functions of the vibration frequency at the granulator basket rotation velocity of n = 60 rpm, load of 37 t/h and 1.2 mm hole diameter

The monodispersion process introduces a fundamental improvement in the fertilizer production technology. Use of uniform (monodisperse) granules, for example in agriculture, provides even distribution of the fertilizer on the fertilized area resulting in additional yields up to 10 % [10-12].

Vibrating granulators provide production of strong monodisperse granules with a smooth glossy surface (the monodispersity degree is up to 99 %). Thus, these devices open possibilities to intensify the granulation process and essentially improve the agrotechnical value of fertilizers.

Table 2 shows a comparative analysis of granulometric compositions of final products obtained in different types of granulators.

The improved granulator has following advantages over other granulator types (based on literature, *e.g.* [33-37]):

- high safety in operation;
- production of more competitive uniform granules;
- avoidance of product's sticking in towers;
- decrease of dust;
- increase of the agro-technical value of fertilizers.

Table 2. Comparison of granulometric content of products obtained in the improved rotating vibration granulator and in world analogues of the granulation equipment (reprinted with permission from the Processes and Equipment of Chemical and Petroleum Refinery Department, Sumy State University)

Granule size range, mm	Granulometric content of products, %		
	Centrifugal granulator, company "Kreber" (Netherlands) [31]	Acoustics granulator designed by Research Institute at the Chemical plant (Russia) [32]	Improved rotating vibration granulator (this work)
1 - 4	97-99	98-99	more than 99
2 - 4	83-92	85-95	90-97
2 - 3	75-90	80-90	more than 90
2.0 - 2.5	40-50	45-65	more than 80
less than 1	0.8-2.5	0.8-1.5	0.1-0.8

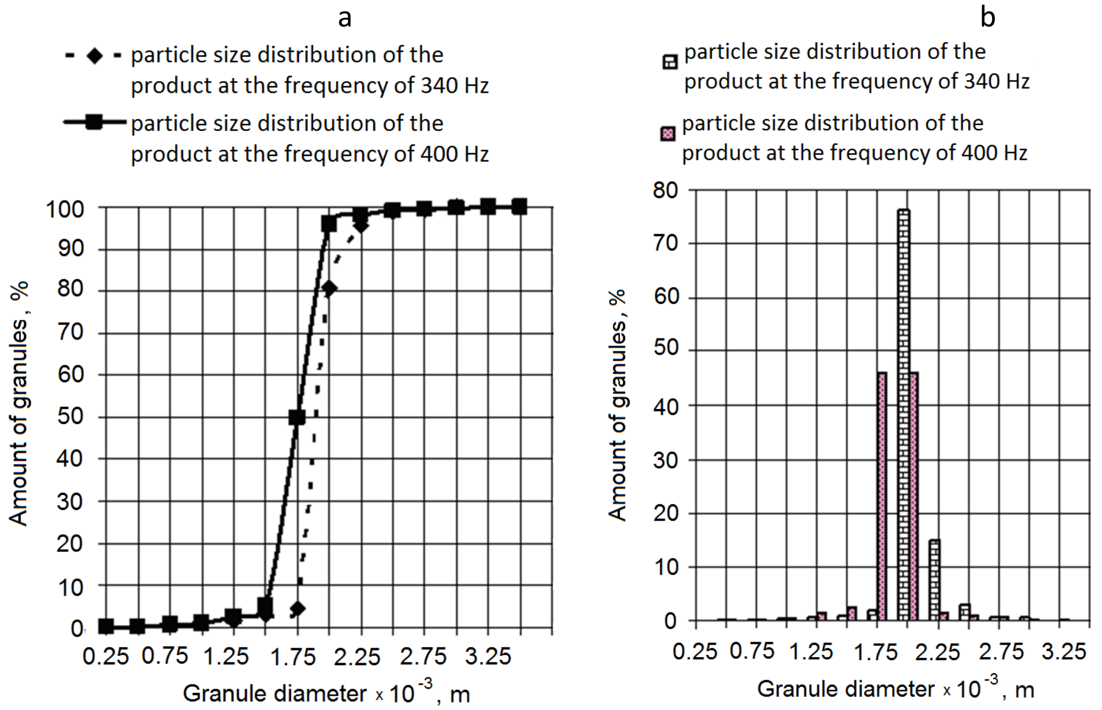

Fig. 9. The integral particle size distribution of ammonium nitrate granules at vibration frequencies of 340 and 400 Hz and the granulator basket rotation velocity of n = 60 rpm, load of 37 t/h and the hole diameter of 1.2 mm: a) line graph b) bar chart

The improved vibrating granulators have a reliable vibration system, which provides a stable imposition of oscillations on fluid jets flowing out of perforated shell holes, regardless the changes in the load on the melt disperser. This vibration system provides measurements of the level of melt in the granulator and thereby, control of the clogging degree and melt outflow velocity from the holes of the perforated shell.

The improved vibrating granulator (Fig. 6) with an electromagnetic vibration system (vibration frequency of 340 Hz) provided production of a product with the following granulometric composition as mass fractions: 0.02 - 0.2 % of granules < 1.0 mm and over 96 % of granules 2.0 - 4.0 mm in size. Also, the fraction of granules in the size range 2.0 - 2.5 mm was not lower than 88 % with the main size in the range 2.1 - 2.5 mm. When the vibration frequency was changed to 400 Hz, the granulator provided a product with the main granule fraction (over 65 %) in the size range 2.5 - 3.0 mm with a simultaneously obtained increased granule hardness (the hardness value was confirmed in [12]).

Similar granulometric compositions of products were obtained by using vibrating granulators with electromagnetic vibration systems in the ammonium nitrate production at tropical conditions in Cuba and in urea production with hydrohumates as foaming additives [12]. During the industrial operation over one month the product (urea) was stably obtained with the following granulometric composition in mass fractions: 0.1 - 0.3 % of granules < 1.0 mm, 99.7 - 99.9 % of granules in the size range 1.0 - 4.0 mm where granules in the size range 2.0 - 4.0 mm comprised 96.5 - 98.9 % while granules larger than 4.0 mm were absent.

4. CONCLUSION

Consideration of hydrodynamic parameters of the liquid jet flowing out of holes of a perforated membrane allowed us to affect the process of jet decay into drops and resulting drop size and dispersity and consequently to improve the construction of a nitrogen fertilizers melt granulator.

Main results:

- a mathematical model was derived to calculate hydrodynamic properties of the melt jet expiration process from a perforated shell;
- influences of the hole diameter and melt properties on the radial velocity field were determined and shown;
- optimal conditions for prilling in a rotating vibration granulator for a given capacity of 37 t/h are defined: the rotation velocity of the basket (60 rpm), the diameter of holes in the perforated shell (1.2 mm), the melt temperature (185 °C), the frequency range of the actuator’s oscillation (340-400 Hz);
- the experimental studies and mathematical modeling provided possibilities for construction of a modernized rotating vibration granulator;
- industrial tests of the modernized vibrating granulator confirmed optimal conditions of the prilling resulting in the improved product.

SYMBOLS

A_1, A_2, A_3	– coefficients of parabolic equation
C_1	– differential equation solution constant
d_{dr}	– diameter of drop, m
d_{dr}^{max}, d_{dr}^{min}	– bigger and smaller diameter of drops, m
Δd_{dr}^{ab}	– absolute difference of drop diameters, m
Δd_{dr}^{rel}	– relative deviation of drop diameters
$F_1(z)$	– polynomial function
f_1, f_2	– upper and lower limits of frequency, s^{-1}
f_{avi}	– average frequency of vibration, which provides monodisperse jets decay, s^{-1}
g	– acceleration of gravity, m s^{-2}
G_S	– melt flowrate, m^3 s^{-1}
G_τ	– the measured volume of the melt, m^3
H	– liquid column height (head), m
n	– number of measurements; granulator basket rotation velocity, rpm
p	– the outflow jet pressure, Pa
p_0	– pressure of the surrounding environment, Pa
r	– radius of the jet, m
t	– the Student’s criterion

V	– velocity of the liquid leaking from the granulator holes, m s^{-1}
$\bar{X}$	– arithmetic mean value
x	– single parameter value
z_0	– initial axial distance, holes, m
z	– axial distance, holes, m
Δ	– maximum possible error of a single measurement, %;
ε	– bilateral confidence interval of the arithmetic mean value
λ_{max}, λ_{min}	– maximum and minimum lengths of the wave, m
ρ	– liquid density, kg m^{-3}
σ	– root-mean-square deviation
τ	– the experimental time of melt outflow through the granulator hole, s.
υ_ϑ υ_r, υ_z	– tangential, radial and axial components of the jet velocity respectively, m s^{-1}
υ_{z_0}	– initial axial component of the jet velocity respectively, m s^{-1}
φ	– discharge coefficient

Acknowledgements: *The authors thank researchers at the Processes and Equipment of Chemical and Petroleum Refinery Department, Sumy State University and the Department of Numerical Methods and Computational Modeling, Alexander Dubcek University of Trencin for their valuable comments during the article preparation.*

This research work had been supported by the Cultural and Educational Grant Agency of the Slovak Republic (KEGA), project No. KEGA 002TnUAD-4/2019 and by the Ministry of Science and Education of Ukraine under the project «Small-scale energy-saving modules with the use of multifunctional devices with intensive hydrodynamics for the production, modification and encapsulation of granules», project No. 0119U100834.

REFERENCES

[1] Feng L, Liu M, Wanga J, Sunc J, Wanga J, Maoa Y. Study on the flow instability of a spray granulation tower. *Sep Purif Technol*. 2016; 169:210−222.

[2] Artyukhov AE, Obodiak VK, Boiko, PG, Rossi PC. Computer modeling of hydrodynamic and heat-mass transfer processes in the vortex type granulation devices. *CEUR Workshop Proceedings.* 2017; 1844: 33-47.

[3] Artyukhov AE, Sklabinskyi VI. Hydrodynamics of gas flow in small-sized vortex granulators in the production of nitrogen fertilizers. *Chem Chem Technol.* 2015; 9(3): 337-342.

[4] Urea Casale S.A. [E-text type]. Location of document: http://www.casale.ch/. date of access 22.09.2019

[5] Kahl Group [E-text type]. Location of document: http://www.amandus-kahl-group.de. date of access 22.09.2019

[6] Stamicarbon [E-text type]. Location of document: http://www.stamicarbon.ru. date of access 22.09.2019

[7] Toyo Engineering Corporation [E-text type]. Location of document: http://www.toyo-eng.com. date of access 22.09.2019

[8] Glatt Innovative Technologies for Granules and Pellets [[E-text type]. Location of document: http://www.glatt.com. date of access 22.09.2019

[9] Artyukhov AE, Sklabinskyi VI. Theoretical analysis of granules movement hydrodynamics in the vortex granulators of ammonium nitrate and carbamide production. *Chem Chem Technol*. 2015; 9(2): 175−180.

[10] Sklabinskyi VI, Skydanenko MS., Kononenko NP. Technical audit of melt granulation knots in the production of mineral fertilizers using tower method. *Tech Aud Prod Res.* 2014; 3(2): 16−23.

[11] Norsk Hydro [E-text type]. Location of document: https://www.hydro.com/en

[12] Sklabinskyi VI, Artyukhov AE, Kononenko MP, Rossi PC. Quality improvement of granular nitrogen fertilizer in the prilling plants. In *CLICAP 2015: Congreso Latinoamericano de Ingeniería y Ciencias Aplicadas. Argentina*, 2015, pp. 611-618.

[13] Wu Y, Bao C, Zhou Y. An Innovated Tower-fluidized Bed Prilling Process. *Chin J Chem. Eng*. 2007; 15: 424–428.

[14] Saleh SN, Ahmed SM, Al-mosuli D, Barghi S. Basic design methodology for a prilling tower. *Can J Chem Eng.* 2015; 93: 1403–1409.

[15] Gezerman AO, Corbacioglu BD. New approach for obtaining uniform-sized granules by prilling process. *Chem Eng Elixir Chem Eng.* 2011; 40: 5225–5228.

[16] White F. *Fluid Mechanics.* Kindle Edition; 2015.

[17] Cengel YA, Cimbala JM. *Fluid Mechanics.* Special India; 2016.

[18] Harris FE. *Mathematics for Physical Science and Engineering: Symbolic Computing Applications in Maple and Mathematica*, Academic Press; 2014.

[19] Hannan Z. *wxMaxima for Calculus I.* Zachary Hannan; 2015.

[20] Hannan Z. *wxMaxima for Calculus II*. Zachary Hannan; 2015.

[21] Vibrating granulator. Technical and commercial offer [E-text type]. Location of document: http://pohnv.teset.sumdu.edu.ua/uk/research/know-how.html (in Ukrainian) date of access 22.09.2019
[22] Barsky E. *Entropic Invariants of Two-Phase Flows.* Amsterdam: Elsevier; 2015.
[23] Artyukhov A, Sklabinskiy V., Ivaniia A. Electrical intelligent system for controlling the formation of monodisperse droplets in granulation devices based on magnetostrictive actuator. Proceedings of the International Conference on Modern Electrical and Energy Systems (MEES 2017). 2017; 280-283.
[24] Holin BG . Centrifugal and vibratory granulators and liquid sprayers. Moscow: Mashinostroenie, 1977. (in Russian)
[25] Schulz HE. *Hydrodynamics – Concepts and Experiments.* InTech; 2015.
[26] Sahoo P. Probability and mathematical statistics. University of Louisville; 2013.
[27] Shao J. Mathematical Statistics. Springer-Science+Business Media; 2003.
[28] Rice JA. Mathematical Statistics and Data Analysis. Duxbury: Thomson Brooks/Cole; 2010.
[29] Pradyot P. Handbook of Inorganic Chemicals. McGraw-Hill; 2002
[30] Afanasyev VN. About some features of droplet flows Thermophysics of high temperatures.1998; 36(1): 94–101. (in Ukrainian)
[31] Kreber [E-text type]. Location of document: https://www.kreber.nl/markets/prilling-nitrates date of access 22.09.2019
[32] Research Institute at the Chemical plant [E-text type]. Location of document: https://www.niichimmash.ru/ date of access 22.09.2019
[33] Bin L, Zhongping X, Huixun L, Carlessi L. Prilling tower and process, in particular for producing urea WO No 2014/060951, 2014.
[34] Snyder DM, Rizzi E. Granulation apparatus. IN No 224039, 2008.
[35] Rizzi E. Granulation Process and Apparatus. 2010/0289165, 2010.
[36] Bugarova Z, Polak A, Batyka D, Papp J. Process of preparation of granulated ammonium nitrate-sulphate fertilizer. EP No 1595860, 2010.
[37] Artyukhov AE, Sklabinskyi VI. Experimental and industrial implementation of porous ammonium nitrate producing process in vortex granulators. *Nauk Visn Nats Hirn Univ.* 2013; 6: 42–48.

SAŽETAK

Narušavanje toka rastopa tokom disperzije u uređajima za granulaciju

Vsevolod I. Sklabinskiy[1], Artem E. Artyukhov[1], Mykola P. Kononenko[1], Jan Krmela[2]

[1]*Sumy State University, Sumy, Ukraine*
[2]*Alexander Dubcek University of Trencin, Trencin, Slovak Republic*

(Naučni rad)

Cilj rada je teorijski opis i eksperimentalno proučavanje procesa isticanja mlaza iz perforirane membrane vibracionog granulatora. Matematičko modelovanje hidrodinamike protoka je izvedeno na osnovu klasične mehanike fluida i tehničke hidromehanike. Pouzdanost dobijenih eksperimentalnih rezultata je bazirana na primeni vremenski testiranih metoda u praksi. Dobijena su hidrodinamička svojstva mlaza tečnosti pri isticanju. Predstavljeni matematički model omogućava izračunavanje radijalne komponente brzine isticanja mlaza, kao i određivanje uticaja fizičkih i hemijskih svojstava tečnosti i prečnika otvora na dužinu mlaza i brzinu protoka duž ose do raspršivanja mlaza u kapi. Razvijeni matematički model proširen teorijskim opisom dispergovanja metodom topljenjem iz rotirajućih perforiranih membrana omogućio nam je poboljšanje dizajna granulatora za stabilizaciju hidrodinamičkih parametara toka disperzije. Ispitivan je proces dispergovanja azotnih đubriva metodom topljenja pri proizvodnji u industrijskim razmerama i radni parametri procesa raspršivanja mlaza u kapljice, tako da je optimizovana veličina kapljica i nivo monodisperznosti.

Keywords: raspršivanje mlaza, vibracioni granulator, hidrodinamika toka, dispergovanje metodom topljenja, rotirajuća perforirana membrana